Parametric local stability condition of a multi-converter system

Taouba Jouini[1] and Florian Dörfler[2]

***Abstract*—We study local (also referred to as small-signal) stability of a network of identical DC/AC converters having a rotating degree of freedom. We develop a stability theory for a class of partitioned linear systems with symmetries that has natural links to classical stability theories of interconnected systems. We find stability conditions descending from a particular Lyapunov function involving an oblique projection onto the complement of the synchronous steady state set and enjoying insightful structural properties. Our sufficient and explicit stability conditions can be evaluated in a fully decentralized fashion, reflect a parametric dependence on the converter's steady-state variables, and can be one-to-one generalized to other types of systems exhibiting the same behavior, such as synchronous machines. Our conditions demand for sufficient reactive power support and resistive damping. These requirements are well aligned with practitioners' insights.**

I. Introduction

The major shift in power generation from conventional synchronous machines to renewables led to the study of problems of network stability composed mainly of DC/AC converters mimicking the electro-mechanical interaction of synchronous machines with the grid. Power system stability amounts to the ability of an electric power system, for a given initial operating condition, to regain state of desired operation, after being subjected to a disturbance [2]. Synchronous machines embody mechanical systems having a rotational degree of freedom. As a result, power system dynamics admit trigonometric nonlinearities, diffusive coupling between electrical and mechanical angles and a rotational symmetry. Converters controlled to emulate synchronous machines [3]–[8] endow the closed loop with a virtual rotating angle and thus inherit these dynamics, which are challenging for many stability analysis approaches.

In this context, different power system stability conditions have been proposed: In [6], [9], [10] sufficient stability conditions are obtained for a single-machine/converter case. Typically, the individual generators and converters are designed and controlled to be stable in isolation. Hence, the bulk of the literature focuses on the network case. In [11] a link is drawn between the synchronization of power systems and Kuramoto oscillators resulting in conditions on the system topology and parameters. Although these conditions give qualitative insights into the sensitivities influencing stability, they usually require strong (and often unrealistic) assumptions. Also the conditions in [11] and elsewhere [3], [4], [11], [12] cannot be assessed without an omniscient knowledge of system parameters and the operating point. In general, explicit stability conditions require strong assumptions (e.g., strong mechanical or electrical damping) [7]–[11], whereas implicit conditions are based on semi-definite programs and thus not very insightful [13], [14]. Some conditions are valid only in radial networks [12]. Classical energy function analysis [15] and its modern extensions [16] consider low-order machine models and quasi-stationary lossless line models implying a weak coupling between active versus reactive power as well as voltage angle versus magnitude. These assumptions make the stability analysis tractable but in real power systems rotor angle stability and voltage stability are inevitably coupled, low-order models are not always a truthful representation, and lines have resistive losses and non-negligible dynamics — especially on the shorter time scales and on lower voltage levels relevant for converters [17]. Quite opposing these assumptions, experimental and theoretical findings underscore that sufficient (virtual) resistive damping and reactive power support are necessary for power system stability [18], [19].

In this paper, we consider a higher-order multi-source power system model consisting of identical DC/AC converters interconnected in a general topology through lossy lines with uniform inductive-resistive dynamics. The converters are controlled through matching control [6]–[8] which renders them structurally equivalent to synchronous machines. Thus, our analysis approach also extends to synchronous machines.

Our model exhibits a rotational symmetry corresponding to the absence of an absolute angle. We pursue a parametric linear stability analysis at a synchronous and rotationally invariant steady state. Towards this, we develop a novel analysis approach for a class of partitioned linear systems characterized by a stable subsystem and a one-dimensional invariant subspace. We propose a class of Lyapunov functions characterized by an oblique projection onto the complement of the invariant subspace, following the direction of a matrix to be chosen as solution to Lyapunov and Ricatti equations. Our approach has natural cross-links with analysis concepts for interconnected systems, e.g., passive systems, though our assumptions are less restrictive. For the multi-source power system model, we arrive at explicit stability condition that depend only on the converter's parameters and steady-state values and can thus be evaluated in a fully decentralized fashion. Unlike other works, our conditions do not require the restrictive assumption of overly strong mechanical (respectively DC-side) damping but rather sufficient reactive power support and AC-side resistance.

II. Modeling and Setup

A. DC/AC Converter Model

Consider a balanced three-phase DC/AC converter model, as in [6] and as illustrated in Figure 1. The dynamics, formulated

[1]Taouba Jouini is with the Department of Automatic Control at LTH, Lund University.[2] Florian Dörfler is with Automatic Control Laboratory, ETH Zurich, Switzerland. Emails: taouba.jouini@control.lth.se, doerfler@ethz.ch. A preliminary version of part of the results in this paper was presented at the European Control Conference 2019 [1]. This work was funded by the European Union's Horizon 2020 research and innovation program under grant agreement N° 691800 and ETH Zürich funds.

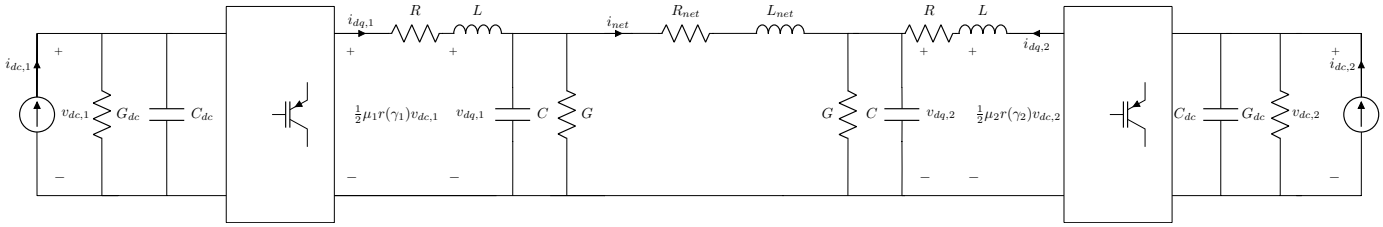

Fig. 1: An example of a graph $\mathcal{G} = (V, \mathcal{E})$ composed of two identical DC/AC converters connected via three RL lines on the AC side, where the node-edge incidence matrix is given by $\mathbf{B} = \begin{bmatrix} -I & I \end{bmatrix}^\top$.

in a rotating frame with angular frequency ω^* are

$$C_{dc}\dot{v}_{dc} = -G_{dc}\, v_{dc} - \tfrac{1}{2} m_{dq}^\top i_{dq} + i_{dc} \tag{1a}$$

$$L\dot{i}_{dq} = -Z_R\, i_{dq} + \tfrac{1}{2} m_{dq} v_{dc} - v_{dq} \tag{1b}$$

$$C\dot{v}_{dq} = -Z_V\, v_{dq} + i_{dq} - i_{net}\,, \tag{1c}$$

where we defined the impedance matrices $Z_R = RI + J\omega^* L \in \mathbb{R}^{2\times 2}$, $Z_V = GI + J\omega^* C \in \mathbb{R}^{2\times 2}$ and used the shorthand $I = \left[\begin{smallmatrix} 1 & 0 \\ 0 & 1 \end{smallmatrix}\right]$, $J = \left[\begin{smallmatrix} 0 & -1 \\ 1 & 0 \end{smallmatrix}\right]$. The DC circuit is represented by its capacitance $C_{dc} > 0$, conductance $G_{dc} > 0$ and a controllable current source $i_{dc} \in \mathbb{R}$. The voltage across the DC capacitor is denoted by $v_{dc} \in \mathbb{R}_{\geq 0}$. The modulation signal, representing the principal converter control input, is given by $m_{dq} \in [-1, +1]^2$ and transforms DC signals into AC signals filtered at the output of the converter via a resistor $R > 0$, an inductor $L > 0$, and a capacitor $C > 0$. The voltage at the output capacitor is denoted by $v_{dq} \in \mathbb{R}^2$, and the current flowing through the inductance is $i_{dq} \in \mathbb{R}^2$. The conductance $G > 0$ models a resistive load attached to the converter at its terminal. The current flowing out from the converter into the network is denoted by $i_{net} \in \mathbb{R}^2$.

Finally, note that (1) is an *averaged* model of the switched converter circuit, where all signals are averaged over a switching period. Such models neglect higher-order switching harmonics and hybrid conversion dynamics but are standard for analysis and control design of grid-connected inverters [20].

The following control is based on the concept of matching the converter model to a synchronous machine; see Remark 1. The converter modulation signal is controlled as a sinusoid with constant magnitude $\mu \in]0, 1[$ and frequency $\dot{\gamma} \in \mathbb{R}$ (relative to ω^*) given by the DC voltage deviation [6]–[8],

$$\dot{\gamma} = \eta\,(v_{dc} - v_{dc}^*) \tag{2a}$$

$$m_{dq} = \mu \begin{bmatrix} -\sin(\gamma) \\ \cos(\gamma) \end{bmatrix}, \tag{2b}$$

where $\gamma \in \mathbb{S}^1$ is the virtual angle, and $\eta > 0$ is a gain.

Next, we design the current source i_{dc} as a combination of a feed-forward term represented by $i_{dc}^* + G_{dc} v_{dc}^*$ and a feedback term on the DC voltage deviation as

$$i_{dc} = i_{dc}^* - K_p\,(v_{dc} - v_{dc}^*) + G_{dc} v_{dc}^*, \tag{3}$$

where $K_p, i_{dc}^* > 0$. The modulation amplitude μ, feedforward current i_{dc}^*, and the control gain K_p are regarded as constants usually determined offline or in outer control loops. Finally, the overall closed-loop DC/AC converter can be written as

$$\dot{\gamma} = \eta\,(v_{dc} - v_{dc}^*) \tag{4a}$$

$$C_{dc}\dot{v}_{dc} = -\hat{K}_p\,(v_{dc} - v_{dc}^*) - \frac{\mu}{2} \begin{bmatrix} -\sin(\gamma) \\ \cos(\gamma) \end{bmatrix}^\top i_{dq} + i_{dc}^* \tag{4b}$$

$$L\dot{i}_{dq} = -Z_R\, i_{dq} + \frac{\mu}{2} \begin{bmatrix} -\sin(\gamma) \\ \cos(\gamma) \end{bmatrix} v_{dc} - v_{dq} \tag{4c}$$

$$C\dot{v}_{dq} = -Z_V\, v_{dq} + i_{dq} - i_{net}\,, \tag{4d}$$

where we used the shorthand $\hat{K}_p = G_{dc} + K_p$.

Remark 1 (Parallels in Synchronous Machines)**.** *Observe that the closed-loop DC/AC converter dynamics* (4) *match one-to-one those of a synchronous machine with single-pole pair, non-salient rotor under constant excitation [6], [7], and thus all the results derived below can conceptually also be applied to synchronous machines; see also Remark 2.* ■

B. Multi-DC/AC converter model

We extend the closed-loop DC/AC converter model (4) to a network of n identical converters interconnected by m identical resistive and inductive lines. With slight abuse of notation, we keep on using the same symbols for parameters and states.

Every closed-loop converter model is as in (4) with identical parameters, modulation signal (2), and connected to the grid through a line with resistance $R_{net} > 0$ set in series with line inductance $L_{net} > 0$. Let B denote the incidence matrix of a connected grid at each phase, then $\mathbf{B} = B \otimes \mathbf{I}$, where $\mathbf{I}$ denote an identity matrix of appropriate dimension. The dynamics of the current i_{net} flowing through the lines are described by $L_{net}\dot{i}_{net} = -Z_{net} i_{net} + \mathbf{B}^\top v_{dq}$, where $Z_{net} = R_{net}\mathbf{I} + \mathbf{J}\omega^* L_{net} \in \mathbb{R}^{2m\times 2m}$. More formally, the n-converter model in vector form is

$$\dot{\gamma} = \eta\,(v_{dc} - v_{dc}^* \mathbb{1}_n) \tag{5a}$$

$$C_{dc}\dot{v}_{dc} = -\hat{K}_p\,(v_{dc} - v_{dc}^* \mathbb{1}_n) - \frac{1}{2}\mathrm{diag}(\mu)\mathbf{R}(\gamma)^\top i_{dq} + i_{dc}^* \tag{5b}$$

$$L\dot{i}_{dq} = -\mathbf{Z}_R\, i_{dq} + \frac{1}{2}\mathbf{R}(\gamma)\,\mathrm{diag}(\mu) v_{dc} - v_{dq} \tag{5c}$$

$$C\dot{v}_{dq} = -\mathbf{Z}_V\, v_{dq} + i_{dq} - \mathbf{B}\, i_{net} \tag{5d}$$

$$L_{net}\dot{i}_{net} = -Z_{net}\, i_{net} + \mathbf{B}^\top v_{dq}\,, \tag{5e}$$

where $\gamma = \begin{bmatrix} \gamma_1, \ldots, \gamma_n \end{bmatrix}^\top \in \mathbb{T}^n$ and $\mathbb{T}^n = \mathbb{S}^1 \times \cdots \times \mathbb{S}^1$ is the n-dimensional torus. We define $v_{dc} =$

$[v_{dc,1}, \ldots, v_{dc,n}]^\top \in \mathbb{R}^n$, $v_{dq} = [v_{dq,1}, \ldots, v_{dq,n}]^\top \in \mathbb{R}^{2n}$, $i_{dq} = [i_{dq,1}, \ldots, i_{dq,n}]^\top \in \mathbb{R}^{2n}$, $i_{net} = [i_{net,1}, \ldots, i_{net,m}]^\top \in \mathbb{R}^{2m}$, and $\mathbf{Z}_R = \mathbf{I} \otimes Z_R \in \mathbb{R}^{2n\times 2n}$, $\mathbf{Z}_V = \mathbf{I} \otimes Z_V \in \mathbb{R}^{2n\times 2n}$, and $\mathbf{R}(\gamma^*) = \operatorname{diag}\{r(\gamma_1^*), \ldots, r(\gamma_n^*)\} \in \mathbb{R}^{2n\times n}$, $r(\gamma_k^*) = \begin{bmatrix} -\sin(\gamma_k^*) \\ \cos(\gamma_k^*) \end{bmatrix} \in \mathbb{R}^2$. An example of two DC/AC converters is shown in Figure 1.

Observe that the dynamics (5) are invariant under a rigid rotation of all AC variables, i.e., under the map

$$\begin{aligned} &\begin{bmatrix} \gamma & v_{dc} & i_{dq} & v_{dq} & i_{net} \end{bmatrix}^\top \mapsto \\ &\begin{bmatrix} \gamma + \theta_0 \mathbb{1}_n & v_{dc} & \mathcal{R}(\theta_0) i_{dq} & \mathcal{R}(\theta_0) v_{dq} & \mathcal{R}(\theta_0) i_{net} \end{bmatrix}^\top \end{aligned} \tag{6}$$

where $\theta_0 \in \mathbb{S}^1$ and $\mathcal{R}(\theta_0)$ is a rotation matrix.

The physical insight is that there is no absolute angle in a power system. We will observe this rotational symmetry also after the linearization.

C. Synchronous steady-state characterization

We are particularly interested in a synchronous steady-state (see Theorem 2 in [21]) with the following properties:

- The frequencies are synchronized at the nominal value ω^* mapped into a nominal DC voltage v_{dc}^*

$$[\omega] = \{\omega \in \mathbb{R}^n_{\geq 0} | \omega = \omega^*\},$$
$$[v_{dc}] = \{v_{dc} \in \mathbb{R}^n_{\geq 0} | v_{dc} = v_{dc}^*\}.$$

- The angles are stationary

$$[\gamma] = \{\gamma \in \mathbb{T}_n | \dot{\gamma}^* = 0\}.$$

- The inductor currents, capacitor voltage and line current are constant at steady state in rotating frame:

$$[i_{dq}] = \left\{i_{dq} \in \mathbb{R}^{2n} | i_{dq}^* = 0\right\},$$
$$[v_{dq}] = \left\{v_{dq} \in \mathbb{R}^{2n} | v_{dq}^* = 0\right\},$$
$$[i_{net,dq}] = \left\{i_{net,dq} \in \mathbb{R}^{2m} | i_{net,dq}^* = 0\right\}.$$

Observe that such a steady state also exhibits the rotational symmetry (6) and thus there is a continuum of steady states.

D. Linearization

We linearize the system equations (5) around a synchronous steady state $x^* = \begin{bmatrix} \gamma^* & v_{dc}^* & i_{dq}^* & v_{dq}^* & i_{net}^* \end{bmatrix}^\top$ leading to

$$\dot{x} = A(x^*)\, x, \tag{7}$$

where x is the difference between the state vector and its steady-state value x^*, the parametric Jacobian matrix is

$$A(x^*) = \left[\begin{array}{cc|ccc} 0 & \eta\mathbf{I} & 0 & 0 & 0 \\ -C_{dc}^{-1}W(x^*) & -C_{dc}^{-1}\hat{K}_P\mathbf{I} & -C_{dc}^{-1}Y(x^*)^\top & 0 & 0 \\ \hline L^{-1}M(x^*) & L^{-1}Y(x^*) & -L^{-1}\mathbf{Z}_R & -L^{-1}\mathbf{I} & 0 \\ 0 & 0 & C^{-1}\mathbf{I} & -C^{-1}\mathbf{Z}_V & -C^{-1}\mathbf{B} \\ 0 & 0 & 0 & L_{net}^{-1}\mathbf{B}^\top & -L_{net}^{-1}\mathbf{Z}_{net} \end{array}\right],$$

$\mathbf{J} = \mathbf{I} \otimes J$, and the block matrices are given by

$$W(x^*) = \tfrac{1}{2}\operatorname{diag}(\mu)\operatorname{diag}\left((\mathbf{J}\mathbf{R}(\gamma^*))^\top i_{dq}^*\right) = \operatorname{diag}(w_k(x_k^*)),$$
$$Y(x^*) = \tfrac{1}{2}\operatorname{diag}(\mu)\mathbf{R}(\gamma^*), M(x^*) = \tfrac{1}{2}\operatorname{diag}(\mu)v_{dc}^*\mathbf{J}\mathbf{R}(\gamma^*).$$

In the Jacobian $A(x^*)$, we have already indicated a suitable partitioning that will be favorable for our latter analysis.

Note that $v(x^*) = \begin{bmatrix} v_1^{*\top} & v_2^{*\top} \end{bmatrix}^\top$, where $v_1^* = \begin{bmatrix} \mathbb{1}_n & 0 \end{bmatrix}^\top$, $v_2^* = \begin{bmatrix} \mathbf{J}i_{dq}^* & \mathbf{J}v_{dq}^* & \mathbf{J}i_{net}^* \end{bmatrix}^\top$ is an invariant subspace of $A(x^*)$, so that

$$A(x^*) \cdot v(x^*) = 0.$$

Observe that the invariant subspace $v(x^*) \in \ker(A(x^*))$ is the tangent vector of the rotational symmetry, i.e., $v(x^*) = \begin{bmatrix} \mathbb{1}_n & 0 & \mathbf{J}i_{dq}^* & \mathbf{J}v_{dq}^* & \mathbf{J}i_{net}^* \end{bmatrix}^\top$ can be obtained by the partial derivative $\partial/\partial\theta_0$ of (6), evaluated at the steady state x^*.

III. Stability of a class of linear systems

In this section, we develop a stability theory for a general class of linear systems enjoying some of the structural properties featured by the system matrix $A(x^*)$ in (7).

A. Separable Lyapunov Analysis for Systems with Symmetries

We consider a class of partitioned linear systems of the form

$$\dot{x} = \left[\begin{array}{c|c} A_{11} & A_{12} \\ \hline A_{21} & A_{22} \end{array}\right] x, \tag{8}$$

where $x = [x_1^\top \; x_2^\top]^\top$ denotes the partitioned state vector, and the block matrices $A_{11}, A_{12}, A_{21}, A_{22}$ are of appropriate dimensions.

In the following, we assume stability of the subsystem characterized by A_{11} and the existence of a symmetry, i.e., an invariant zero eigenspace:

Assumption 1. *The block matrix A_{11} in (8) is Hurwitz.*

Assumption 2. *There exists a vector $v = [v_1^\top \; v_2^\top]^\top$, so that*

$$A \cdot span\{v\} = 0.$$

Assumption 2 is compatible with the nullspace of $A(x^*)$ in (7). However, we remark that all of our analysis holds analogously if this assumption is removed; see Corollary III.4.

We are interested in asymptotic stability of the subspace $\operatorname{span}\{v\}$: all eigenvalues of A should be in the left-half plane except for one at zero, whose eigenspace is $\operatorname{span}\{\mathrm{v}\}$. Recall that the standard stability definitions and Lyapunov methods extend from stability of the origin to stability of closed and invariant sets when using the point-to-set-distance rather than merely the norm in the comparison functions; see e.g., [22, Theorem 2.8]. In our case, we seek a quadratic Lyapunov function that vanishes on $\operatorname{span}\{v\}$, is positive elsewhere and whose derivative is decreasing everywhere outside $\operatorname{span}\{v\}$.

We start by defining an appropriate Lyapunov candidate

$$V(x) = x^\top \left(P - \frac{Pvv^\top P}{v^\top P v}\right) x, \tag{9}$$

where P is *a positive definite* matrix. Our Lyapunov candidate construction is based on two *key* observations:

- First, the function $V(x)$ is defined via an oblique projection of the vector $x \in \mathbb{R}^n$ parallel to $\operatorname{span}\{v\}$ onto $\{x \in \mathbb{R}^n | v^\top P x = 0\}$. If $P = \mathbf{I}$, then V is the *orthogonal projection onto* $\mathcal{X} = \operatorname{span}\{v\}^\perp$. Hence, $V(x)$ vanishes on $\operatorname{span}\{v\}$ and is strictly positive elsewhere.
- Second, the positive definite matrix P is *a degree of freedom* that can be specified later to provide sufficient and favorable (e.g., decentralized) stability conditions.

In standard Lyapunov analysis, one seeks a pair of matrices $(P,\mathcal{Q})$ with suitable positive (semi-)definiteness properties so that the Lyapunov equation $PA+A^\top P=-\mathcal{Q}$ is met. In the following, we apply a helpful twist and parameterize the $\mathcal{Q}$-matrix as a quadratic function $\mathcal{Q}(P)$ of P, which renders the Lyapunov equation to an algebraic Ricatti equation. We choose the following structure for the matrix $\mathcal{Q}(P)$

$$\mathcal{Q}(P)=\begin{bmatrix} Q_1 & H^\top(P) \\ H(P) & H(P)Q_1^{-1}H(P)^\top+Q_2 \end{bmatrix}, \tag{10}$$

where Q_1 is a positive definite matrix, Q_2 is a positive semi-definite matrix with respect to $\operatorname{span}\{v_2\}$, P is block-diagonal,

$$P=\begin{bmatrix} P_1 & 0 \\ 0 & P_2 \end{bmatrix}, \tag{11}$$

with $P_1=P_1^\top>0$ and $P_2=P_2^\top>0$, i.e., the Lyapunov function is *separable*, and finally $H(P)=A_{12}^\top P_1+P_2A_{21}$ is a shorthand.

We need to introduce a third and final assumption.

Assumption 3. *Consider the matrix $F=A_{22}+A_{21}Q_1^{-1}P_1A_{12}$. Assume that the pair $(F,A_{21}Q_1^{-1/2})$ is stabilizable and the pair (F,D) is detectable, where $DD^\top=A_{12}^\top P_1Q_1^{-1}P_1A_{12}+Q_2$.*

Assumption 3 will guarantee suitable definiteness and decay properties of the separable Lyapunov function (11) under comparatively mild conditions, as discussed in Section III-B.

Assumptions 1, 2, and 3 recover our requirement for positive definiteness of the matrix P in (11) and semi-definitness (with respect to $\operatorname{span}\{v\}$) of $\mathcal{Q}(P)$ in (10) as shown in the following.

Proposition III.1. *Under Assumptions 1, 2 and 3, the matrix P in* (11) *is unique and positive definite.*

Proof. By calculating $PA+A^\top P=-\mathcal{Q}(P)$, where A is as in (8), P is as in (11), and $\mathcal{Q}(P)$ is as in (10), we obtain

$$\begin{bmatrix} P_1A_{11}+A_{11}^\top P_1 & H(P)^\top \\ H(P) & P_2A_{22}+A_{22}^\top P_2 \end{bmatrix}=-\begin{bmatrix} Q_1 & H(P)^\top \\ H(P) & H(P)Q_1^{-1}H(P)^\top+Q_2 \end{bmatrix},$$

the block-diagonal terms of which are

① $P_1A_{11}+A_{11}^\top P_1=-Q_1$,
② $P_2A_{22}+A_{22}^\top P_2=-H(P)Q_1^{-1}H(P)^\top-Q_2$.

Since A_{11} is Hurwitz, there is a unique and positive definite matrix P_1 solving ①. Moreover, specification ② is equivalent to solving for P_2 in the following algebraic Riccati equation:

$$P_2A_{21}Q_1^{-1}A_{21}^\top P_2+P_2F+F^\top P_2+A_{12}^\top P_1Q_1^{-1}P_1A_{12}+Q_2=0,$$

where $F=A_{22}+A_{21}Q_1^{-1}P_1A_{12}$. Under Assumption 3, there is a solution to ② with P_2 unique and positive definite. □

Lemma III.2. *Under Assumptions 1, 2 and 3, the matrix $\mathcal{Q}(P)$ in* (10) *is positive semi-definite. Additionally,* $\ker(A)=\ker(\mathcal{Q}(P))=\operatorname{span}\{v\}$.

Proof. First, observe that the matrix $\mathcal{Q}(P)$ in (10) is symmetric and the upper left block $Q_1>0$ is positive definite. By using the Schur complement and positive semi-definiteness of Q_2, we obtain that $\mathcal{Q}(P)$ is positive semi-definite. Second, by virtue of $v^\top\mathcal{Q}(P)v=v^\top(PA+A^\top P)v=0$ due to Assumption 2, it follows that $\operatorname{span}\{v\}\subset\ker(\mathcal{Q}(P))$. Third, consider a general vector $s=\begin{bmatrix}s_1^\top s_2^\top\end{bmatrix}^\top$, so that $\mathcal{Q}(P)s=0$. We obtain the algebraic equations $Q_1s_1+H(P)^\top s_2=0, H(P)s_1+\big(H(P)Q_1^{-1}H(P)^\top+Q_2\big)s_2=0$. One deduces that $Q_2s_2=0$ and thus $s_2\in\operatorname{span}\{v_2\}$. The latter implies $s_1=-Q_1^{-1}H(P)^\top\operatorname{span}\{v_2\}=\operatorname{span}\{v_1\}$ because $\mathcal{Q}(P)\operatorname{span}\{v\}=0$. Thus, it follows that $s\in\operatorname{span}\{\begin{bmatrix}s_1^\top s_2^\top\end{bmatrix}^\top\}=\operatorname{span}\{v\}$ and we deduce that $\ker(\mathcal{Q}(P))=\operatorname{span}\{v\}$. Fourth and finally, for the sake of contradiction, take a vector $\tilde v\notin\operatorname{span}\{v\}$, so that $\tilde v\in\ker(A)\Rightarrow\tilde v^\top\big(A^\top P+PA\big)\tilde v=0\Rightarrow\tilde v^\top\mathcal{Q}(P)\tilde v=0\Rightarrow\tilde v\in\ker(\mathcal{Q}(P))$. This is a contradiction to $\ker(\mathcal{Q}(P))=\operatorname{span}\{v\}$. Hence, we conclude that $\ker(A)=\ker(\mathcal{Q}(P))=\operatorname{span}\{v\}$. □

Next, we provide the main result of this section.

Theorem III.3. *Consider system* (8)*. Under Assumptions 1, 2 and 3, $\operatorname{span}\{v\}$ is an asymptotically stable subspace of A.*

Proof. Consider the function $V(x)$ in (9). The matrix P in (11) is positive definite by Proposition III.1. Take $y=P^{1/2}x$ and $w=P^{1/2}v$, the function $V(x)$ can be rewritten as $V(y)=y^\top\Big(\mathbf{I}-\frac{ww^\top}{w^\top w}\Big)y=y^\top\Pi_w y$. The matrix $\Pi_w=\mathbf{I}-\frac{ww^\top}{w^\top w}$ is a projector into the orthogonal complement of $\operatorname{span}(w)$, and is hence positive semi-definite with one-dimensional nullspace corresponding to $P^{1/2}\operatorname{span}\{v\}$. It follows that the function $V(x)$ is positive semi-definite with respect to $\operatorname{span}\{v\}$. By means of $Av=\mathcal{Q}(P)v=0$ in $v^\top PA=v^\top(\mathcal{Q}-A^\top P)=0$, we obtain $\dot V(x)=-x^\top\mathcal{Q}(P)x$. By Lemma III.2, it holds that $\dot V(x)$ is negative definite with respect to $\operatorname{span}\{v\}$. We apply Lyapunov's method and Theorem 2.8 in [22], to conclude that $\operatorname{span}\{v\}$ is asymptotically stable. □

B. Contextualizing and Relations to Existing Results

In what follows, we consider a few special cases and put Theorem III.3 as well as Assumptions 1, 2 and 3 into context.

First, note that our approach is general and can be applied to matrices that do not have a nullspace as in Assumption 2. In this case, the Lyapunov function (9) is simply chosen as $V(x)=x^\top Px$, with P being positive definite and separable as in (11), Q_1 is positive definite and Q_2 in (10) is chosen to be positive definite. In this case our analysis applies analogously.

Corollary III.4. *Under Assumptions 1 and 3, the linear system* (8) *is asymptotically stable.*

Second, we put Assumption 3 into context and compare it to other system classes admitting separable Lyapunov functions. Towards this, it will be helpful to consider system (8) as an interconnected closed-loop system, as illustrated in Figure 2. For simplicity of presentation, in the remainder of this section, we consider only the case of Corollary III.4, that is, we discard the existence of a nullspace as in Assumption 2. We will also consider only the *sufficient* condition that $F=A_{22}+A_{21}Q_1^{-1}P_1A_{12}$ is Hurwitz which implies Assumption 3.

Classical small-gain interpretation: Let us first provide a qualitative insight into Assumption 3. As in Figure 2, we define the stable (due to Assumption 1) subsystem $\Sigma_1:\dot x_1=A_{11}x_1+u_1$ with state x_1, input $u_1=A_{12}x_2$, and

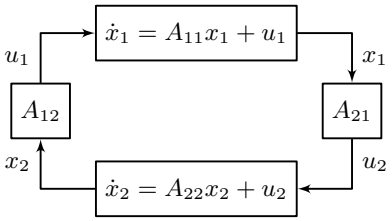

Fig. 2: Illustration of system (8) as interconnected system

output $y_1 = A_{21}x_1$. Recall that if one chooses $Q_1 = 2\gamma \cdot P_1$ with $\gamma > 0$, then P_1 measures the exponential decay[1] of x_1. Now, if A_{22} is Hurwitz as well, then the condition that $F = A_{22} + A_{21}Q_1^{-1}P_1A_{12} = A_{22} + A_{21}A_{12}/(2\gamma)$ is Hurwitz can be understood as a classical small gain condition: A_{11} and A_{22} have to be *sufficiently* stable so that the interconnection through A_{12} and A_{21} remains stable.

Passive systems: The sufficient conditions that A_{11} and F must be Hurwitz include the case of passive systems, which are a well-known class of systems admitting separable Lyapunov functions. To see this, consider again Figure 2, but with a different partitioning. Consider the stable (due to Assumption 1) subsystem $\Sigma_1 : \dot{x}_1 = A_{11}x_1 - A_{12}u_1$ with state x_1, input $u_1 = -x_2$, and output $y_1 = A_{21}x_1$. Consider also the subsystem $\Sigma_2 : \dot{x}_2 = A_{22}x_2 + u_2$ with state x_2, input $u_2 = x_1$, and output $y_2 = x_2$. Assume that both Σ_1 and Σ_2 are strictly passive. Hence, their negative feedback connection is known to be asymptotically stable. Under these conditions it can be shown that A_{11} and F must be Hurwitz. To see this note that, by the Kalman-Yakubovich-Popov (KYP) Lemma, Σ_1 is strictly passive with input u_1 and output y_1 if and only if there are positive definite matrices P_1 and Q_1 so that $P_1A_{11} + A_{11}^\top P_1 = -Q_1$ (which equals Assumption 1) and $-P_1A_{12} = A_{21}^\top$. Likewise, by the KYP Lemma, Σ_2 is strictly passive with input u_2 and output y_2 if and only if the associated storage function is $x^\top P_2 x = x^\top x$, that is, A_{22} is negative definite. In this case, $F = A_{22} + A_{21}Q_1^{-1}P_1A_{12} = A_{22} - A_{21}Q_1^{-1}A_{21}^\top$ is negative definite (Hurwitz), and Assumptions 1 and 3 are satisfied.

IV. Local stability of the multi-DC/AC converter

This section sets the first milestone towards characterizing the stability of nonlinear multi-converter systems. Ultimately, we seek to answer the question: under which conditions is the synchronous steady state set locally asymptotically stable? For this, we apply the theory developed in the previous section to give nuts and bolts on how to derive sufficient parametric conditions for the closed-loop multi-converter model (5). We consider the linearized model (7) and identify the matrices

$$A_{11} = \begin{bmatrix} 0 & \eta\mathbf{I} \\ -C_{dc}^{-1}W(x^*) & -C_{dc}^{-1}K_p\mathbf{I} \end{bmatrix}, A_{12} = \begin{bmatrix} 0 & 0\,0 \\ -C_{dc}^{-1}Y(x^*)^\top & 0\,0 \end{bmatrix},$$
$$A_{21} = \begin{bmatrix} L^{-1}M(x^*) & L^{-1}Y(x^*) \\ 0 & 0 \\ 0 & 0 \end{bmatrix}, A_{22} = \begin{bmatrix} -L^{-1}\mathbf{Z}_R & -L^{-1}\mathbf{I} & 0 \\ C^{-1}\mathbf{I} & -C^{-1}\mathbf{Z}_V & -C^{-1}\mathbf{B} \\ 0 & L_{net}^{-1}\mathbf{B}^\top & -L_{net}^{-1}\mathbf{Z}_{net} \end{bmatrix}.$$

[1]Indeed, the Lyapunov inequality $P_1A_{11} + A_{11}^\top P_1 \preceq -Q_1$ reduces in this case to $P_1(A_{11} + \gamma I) + (A_{11} + \gamma I)^\top P_1 \preceq 0$ implying that $(A_{11} + \gamma I)$ is stable, or equivalently that A_{11} has all its poles to the left of $-\gamma$.

Define the Lyapunov function $V(x)$ as in (9) with $v = v(x^*)$. Hence, $V(x)$ is positive semi-definite with respect to $\text{span}\{v(x^*)\}$. Next, we fix the matrix $\mathcal{Q}(P)$ given by (10), where we set $Q_1 = \mathbf{I}$, $Q_2 = \mathbf{I} - v_2^* v_2^{*\top}/v_2^{*\top} v_2^*$ and search for the corresponding matrix P so that $PA(x^*) + A^\top(x^*)P = -\mathcal{Q}(P)$.

Analogous to (11), we choose the block diagonal matrix

$$P = \left[\begin{array}{cc|c} P_{11} & P_{12} & 0 \\ P_{12} & P_{22} & 0 \\ \hline 0 & 0 & P_{33} \end{array}\right] = \left[\begin{array}{c|c} P_1 & 0 \\ \hline 0 & P_2 \end{array}\right], \qquad (12)$$

where P_{11}, P_{12} and P_{22} are again chosen to be block diagonal. Notice that the chosen structure of P_1 and the zeros in the off-diagonals in P originates from the physical intuition of the tight coupling between the angle of the converter and its corresponding DC voltage (proportional to the AC frequency), as enabled by the matching control (2). The same type of coupling comes into play in synchronous machines between the rotor angle and its frequency, due to the presence of the electrical power in the swing equation [2]. The 4×4 matrix P_2 is dense with off-diagonals coupling at each phase the inductance current of one converter to the other and vice versa.

In the sequel, we show that this structure allows for sufficient and fully decentralized stability conditions.

Assumption 4 (Parametric Synchronization Condition)**.** *Assume the following condition is satisfied, for all $k \in \{1, \ldots, n\}$,*

$$Q_{x,k}^* > \frac{\mu_k^{*2} v_{dc}^{*2}}{16R}, \qquad (13)$$

where $Q_{x,k}^* = w_k(x_k^*)v_{dc}^*$ is the reactive power output.

Next, we provide the main result of this section.

Theorem IV.1 (Asymptotic Stability)**.** *Consider the linearized closed-loop multi-converter model* (7)*. Under Assumption 4, the subspace span$\{v(x^*)\}$ is asymptotically stable.*

Proof. Since $v(x^*) \in \ker(A)$, Assumption 2 is satisfied. If Assumption 4 is true, then $w_k(x_k^*) > 0$, the submatrix A_{11} is Hurwitz, and Assumption 1 is also valid. Next, we verify Assumption 3: First, the matrix P_1 can be identified from specification ① with $Q_1 = \mathbf{I}$ by

$$P_{11} = \frac{1}{\eta}\left[\hat{K}_p \frac{W(x^*)^{-1}}{2} + \frac{W(x^*)}{2\hat{K}_p}(\mathbf{I} + \eta C_{dc} W(x^*)^{-1})\right],$$
$$P_{12} = P_{12}^\top = \frac{1}{2}W(x^*)^{-1}C_{dc}, P_{22} = \frac{C_{dc}}{2\hat{K}_p}\left(\mathbf{I} + \eta C_{dc} W(x^*)^{-1}\right).$$

The feasibility of specification ② with the positive semi-definite matrix $Q_2 = \mathbf{I} - \frac{v_2^{*\top} v_2^*}{v_2^{*\top} v_2^*}$ is given by

$$P_2 A_{21} A_{21}{}^\top P_2 + P_2 F + F^\top P_2 + SS^\top + Q_2 = 0,$$

where $F = A_{22} + A_{21}P_1A_{12}$, and $S = A_{12}^\top P_1$. If F is Hurwitz, then (F, A_{21}) is stabilizable and (F, D) is detectable, where $DD^\top = SS^\top + Q_2$.

Next, we find sufficient and fully decentralized conditions, for which F satisfies the Lyapunov equation

$FP_F + P_F F = -Q_F$. We choose P_F and Q_F to be block-diagonal matrices $P_F = \begin{bmatrix} L & 0 & 0 \\ 0 & C & 0 \\ 0 & 0 & L_{net} \end{bmatrix}$, $Q_F = \begin{bmatrix} \Gamma & 0 & 0 \\ 0 & 2G\mathbf{I} & 0 \\ 0 & 0 & 2R_{net}\mathbf{I} \end{bmatrix}$, with $\Gamma = 2R\mathbf{I} + C_{dc}^{-1}\left(M(x^*)P_{12}Y(x^*)^\top + Y(x^*)P_{12}M(x^*)^\top\right) + 2C_{dc}^{-1}\left(Y(x^*)P_{22}Y(x^*)^\top\right)$ being itself block-diagonal. Aside from Γ, all diagonal blocks of P_F and Q_F are positive definite. We evaluate the block-diagonal matrix Γ for positive definiteness by exploring its two-by-two block diagonals, where trace and determinant of each block are positive under Assumption 4. By applying Theorem III.3, we deduce that $\text{span}\{v(x^*)\}$ is asymptotically stable for the linearized system (7). □

While our stability analysis is formally valid only for the invariant subspace $\text{span}\{v(x^*)\}$ of the linearized model (7), Lyapunov methods in the quotient space (resulting from identifying points induced by the rotational invariance (6) with one another), suggest that the corresponding nonlinear steady state set (5) is locally asymptotically stable. In the next section, we explore via simulations to which extent $V(x)$ actually serves as a Lyapunov function for the nonlinear system (5).

Remark 2 (Evaluation, interpretation, and satisfaction)**.** *Condition* (13) *can be evaluated in a fully decentralized fashion and depends on the converter's resistance R, modulation amplitude* μ*, nominal DC voltage* v_{dc}^**, and reactive power output* Q_x^**. Condition* (13) *requires stability of each individual converter DC system (Assumption 1), which is reasonable since every subsystem is designed to be stable in isolation, and it requires sufficient reactive power support and resistive damping (to meet Assumption 3), which are well-known practical stability conditions [18]. In fact, the sufficient resistive damping is often enforced by virtual impedance control. A simple implementation thereof, is based on the modulation*

$$m' = m + 2k_m \cdot i_{dq} / v_{dc},$$

where m is a vector whose components are as in (2)*,* $k_m > 0$ *is a control gain and the DC voltage is assumed to be non-zero. This virtual impedance control adds* k_m *to the resistance R in* (5c)*, but it also affects the DC dynamics* (5b)*. To counteract the latter, the DC current source is controlled as* $i'_{dc} = i_{dc} + k_m i_{dq}^\top i_{dq}/v_{dc}$*, with* i_{dc} *as in* (3)*. A robust alternative to the feed-forward term* $k_m i_{dq}^\top i_{dq}/v_{dc}$ *in practice is PI-control or high-gain P-control of* i_{dc}*.*

In a more general setting with heterogeneous converter and RL- lines parameters, an analogous condition can be obtained. The analogous stability condition (see Remark 1) for a multi-machine power system is

$$Q_x^* > \frac{L_m^2 i_f^2 \omega^{*2}}{4R},$$

where Q_x^* *is the reactive power output neglecting stator losses,* L_m *is the mutual inductance, and* i_f *is the constant rotor excitation current. This condition sets an upper bound on the back electromotive force dependent on the reactive power and the stator resistance [10]. Observe that the mechanical damping (equivalent to* $\hat{K}_p$ (5)*) has no effect on local stability contrary to many other stability conditions [6], [9]–[11].* ■

V. Simulations

We consider two DC/AC converters in closed-loop with the matching control as described by (5) and connected via an RL line, as depicted in Figure 1. Table I shows the parameters (in p.u.) of the two converters and their controls. We additionally added a reactive load of value $b = 1.3$ (p.u.) in parallel with the resistive load G accounting for, e.g. motors. Next, by means of simulations, we assess the local asymptotic stability of the system and validate the sufficient parametric condition in (13).

	Converter 1	Converter 2	RL Line
i_{dc}^*	5	5	–
v_{dc}^*	1000	1000	–
C_{dc}	10^{-3}	10^{-3}	–
G_{dc}	10^{-5}	10^{-5}	–
η	0.0003142	0.0003142	–
L	$5 \cdot 10^{-4}$	$5 \cdot 10^{-4}$	–
C	10^{-5}	10^{-5}	–
μ^*	0.33	0.33	–
G	0.01	0.01	–
b	1.3	1.3	–
K_p	0.099	0.099	–
R_{net}	–	–	0.2
L_{net}	–	–	$5 \cdot 10^{-5}$
R	0.2	0.2	–

TABLE I: Parameter values of the DC/AC converters (in p.u.).

Figure 3 shows a projection of the level sets of the Lyapunov function (9) into $(\gamma_1 - \gamma_1^*, \gamma_2 - \gamma_2^*)$-space (with coordinates shifted relative to the steady state), where $v(x^*) = \begin{bmatrix} v_1(x^*) & v_2(x^*) \end{bmatrix}^\top \in \ker(A(x^*))$, $v_1(x^*) = \begin{bmatrix} 0.043, & 0.043, & 0, & 0 \end{bmatrix}^\top$, and $v_2(x^*) = \begin{bmatrix} -0.0033 & -0.0023 & -0.0033 & -0.0023 & -0.7034 & -0.0108 & -0.7034 & -0.0108 & 0 & 0 \end{bmatrix}^\top$ for a corresponding matrix $P > 0$ as defined in (12). We assure that the parametric condition (13) is met, initialize sample trajectories of the nonlinear two-converter model at various initial conditions x_0, and search for the largest sublevel set $\Omega_c(x^*) = \{x \in \mathbb{R}^{14} | V(x) \leq c\}$ that encloses an estimate of the region of attraction. The found value $c = 1.6121 \cdot 10^4$ is rather large, as it allows for severe transients in voltage angles and magnitudes that will likely not be encountered during regular system operation; see Figures 3-4.

We observe that a projection of the nonlinear steady state set, defined in Section II-C, into the angle space (relative to their steady state) represented by $\text{span}\{\mathbb{1}_2\}$, is forward invariant and attractive within $\Omega_c(x^*)$. Our simulation show also that the rest of the states, namely $[v_{dc}, i_{dq}, v_{dq}, i_{net}]$, converge to a corresponding steady state on the frequency-synchronized manifold. Figure 4 shows indicative voltage trajectories initialized at the boundary of $\Omega_c(x^*)$.

VI. Conclusions

We derived sufficient and fully decentralized conditions for local asymptotic stability of a synchronous steady state of a power system composed of identical DC/AC converters in closed-loop with the matching control. We explored techniques from Lyapunov theory to analyze the small-signal trajectories

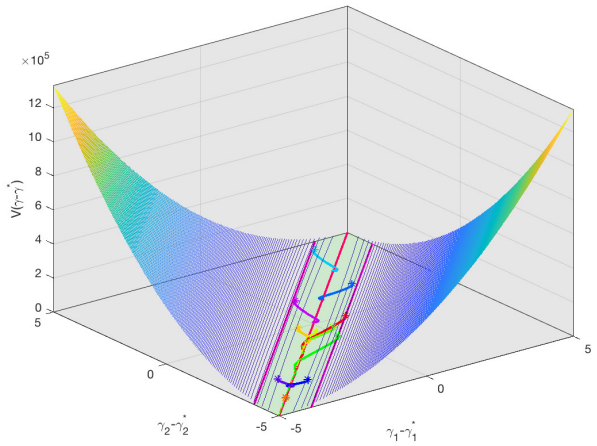

Fig. 3: Projection of the Lyapunov function $V(x)$ into $(\gamma_1 - \gamma_1^*, \gamma_2 - \gamma_2^*)$ space for $P > 0$ as in (12) and the vector $v(x^*)$. The projection of the sublevel set $\Omega_c(x^*)$ for $c = 1.6121 \cdot 10^4$ is colored in green. Sample nonlinear trajectories of (5) satisfying condition (13) and originating within $\Omega_c(x^*)$ (with initial conditions marked by stars) show that the nonlinear steady state set is locally asymptotically stable.

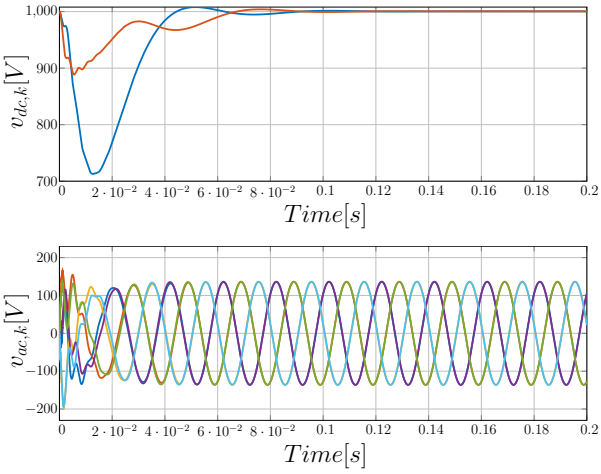

Fig. 4: Time-domain simulations showing synchronization of the DC and AC voltages $v_{dc,k}$ and $v_{ac,k}$, $k = \{1,2\}$ for trajectories starting on the boundary of the sublevel set $\Omega_c(x^*)$.

of the system, where the basic idea is to resort to oblique projection, while exploiting the different degrees of freedom of the proposed Lyapunov function. We established a stability theory that encompasses a class of linear systems inspired by our problem statement and that coalesce into well-known concepts for stability of interconnected systems. Venues for future work include a formal characterization of local asymptotic stability, the study of conservativeness of our parametric condition and a semi-global analysis of systems with rotational symmetry.

References

[1] T. Jouini and F. Dörfler, "Local synchronization of two dc/ac converters via matching control," in *2019 18th European Control Conference (ECC)*. IEEE, 2019, pp. 2996–3001.

[2] P. Kundur, *Power system stability and control*. McGraw-Hill, 1994.

[3] M. Colombino, D. Groß, J. Brouillon, and F. Dörfler, "Global phase and magnitude synchronization of coupled oscillators with application to the control of grid-forming power inverters," *IEEE Transactions on Automatic Control*, vol. 64, no. 11, pp. 4496 – 4511, February 2019.

[4] D. Groß, M. Colombino, J. Brouillon, and F. Dörfler, "The effect of transmission-line dynamics on grid-forming dispatchable virtual oscillator control," *IEEE Transactions on Control of Network Systems*, vol. 6, no. 3, pp. 1148–1160, September 2019.

[5] B. B. Johnson, S. V. Dhople, A. O. Hamadeh, and P. T. Krein, "Synchronization of parallel single-phase inverters with virtual oscillator control," *IEEE Transactions on Power Electronics*, vol. 29, no. 11, pp. 6124–6138, 2014.

[6] C. Arghir, T. Jouini, and F. Dörfler, "Grid-forming control for power converters based on matching of synchronous machines," *Automatica*, vol. 95, pp. 273–282, 2018.

[7] C. Arghir and F. Dörfler, "The electronic realization of synchronous machines: model matching, angle tracking and energy shaping techniques," *IEEE Transactions on Power Electronics*, 2019, In press. DOI 10.1109/TPEL.2019.2939710.

[8] S. Curi, D. Groß, and F. Dörfler, "Control of low-inertia power grids: A model reduction approach," in *IEEE 56th Annual Conference on Decision and Control (CDC)*. IEEE, 2017, pp. 5708–5713.

[9] S. Y. Caliskan and P. Tabuada, "Compositional transient stability analysis of multimachine power networks," *IEEE Transactions on Control of Network systems*, vol. 1, no. 1, pp. 4–14, 2014.

[10] N. Barabanov, J. Schiffer, R. Ortega, and D. Efimov, "Almost global attractivity of a synchronous generator connected to an infinite bus," in *IEEE 55th Conference on Decision and Control (CDC)*. IEEE, 2016, pp. 4130–4135.

[11] F. Dörfler and F. Bullo, "Synchronization and transient stability in power networks and nonuniform kuramoto oscillators," *SIAM Journal on Control and Optimization*, vol. 50, no. 3, pp. 1616–1642, 2012.

[12] F. Dörfler, J. W. Simpson-Porco, and F. Bullo, "Breaking the hierarchy: Distributed control and economic optimality in microgrids," *IEEE Transactions on Control of Network Systems*, vol. 3, no. 3, pp. 241–253, 2016.

[13] J. Schiffer, D. Efimov, and R. Ortega, "Global synchronization analysis of droop-controlled microgrids–a multivariable cell structure approach," *Automatica*, vol. 109, p. 108550, 2019.

[14] T. L. Vu and K. Turitsyn, "Lyapunov functions family approach to transient stability assessment," *IEEE Transactions on Power Systems*, vol. 31, no. 2, pp. 1269–1277, 2016.

[15] H.-D. Chiang, C.-C. Chu, and G. Cauley, "Direct stability analysis of electric power systems using energy functions: theory, applications, and perspective," *Proceedings of the IEEE*, vol. 83, no. 11, pp. 1497–1529, 1995.

[16] L. Zhu and D. J. Hill, "Stability analysis of power systems: A network synchronization perspective," *SIAM Journal on Control and Optimization*, vol. 56, no. 3, pp. 1640–1664, 2018.

[17] F. Milano, F. Dörfler, G. Hug, D. J. Hill, and G. Verbič, "Foundations and challenges of low-inertia systems," in *2018 Power Systems Computation Conference (PSCC)*. IEEE, 2018, pp. 1–25.

[18] X. Wang, Y. W. Li, F. Blaabjerg, and P. C. Loh, "Virtual-impedance-based control for voltage-source and current-source converters," *IEEE Transactions on Power Electronics*, vol. 30, no. 12, pp. 7019–7037, 2015.

[19] P. Vorobev, P. Huang, M. A. Hosani, J. L. Kirtley, and K. Turitsyn, "Towards plug-and-play microgrids," in *IECON 2018 - 44th Annual Conference of the IEEE Industrial Electronics Society*, Oct 2018, pp. 4063–4068.

[20] A. Yazdani and R. Iravani, *Voltage-sourced converters in power systems*. Wiley Online Library, 2010, vol. 34.

[21] D. Groß, C. Arghir, and F. Dörfler, "On the steady-state behavior of a nonlinear power system model," *Automatica*, vol. 90, pp. 248–254, 2018.

[22] Y. Lin, E. D. Sontag, and Y. Wang, "A smooth converse lyapunov theorem for robust stability," *SIAM Journal on Control and Optimization*, vol. 34, no. 1, pp. 124–160, 1996.